INTERNATIONAL JOURNAL OF HYDROGEN ENERGY 41 (2016) 22886–22898

Available online at www.sciencedirect.com

ScienceDirect

journal homepage: www.elsevier.com/locate/he

Adsorption and dissociation of H_2 on Pd doped graphene-like SiC sheet

Masoud Bezi Javan [a,*], *Amir Houshang Shirdel-Havar* [b], *Alireza Soltani* [c], *Faiz Pourarian* [d]

[a] *Physics Department, Faculty of Sciences, Golestan University, Gorgan, Iran*
[b] *Institute of Physics, Kazan Federal University, Kazan, Russian Federation*
[c] *Golestan Rheumatology Research Center, Golestan University of Medical Sciences, Gorgan, Iran*
[d] *Department of Materials Science and Engineering, Carnegie Mellon University, Pittsburgh, PA, USA*

ARTICLE INFO

Article history:
Received 26 June 2016
Received in revised form
2 September 2016
Accepted 12 September 2016
Available online 6 October 2016

Keywords:
SiC
Pd
Hydrogen
Adsorption
Dissociation
DFT

ABSTRACT

Doped porous SiC nanostructures with metallic atoms, nanoclusters and nanoparticles have been recognized as promising materials for hydrogen storage. With this regards transition metal elements are interesting impurities for use as doping. In view of this prospect, a theoretical approach based on density functional theory (DFT) was applied to study of the interaction between hydrogen molecule and a graphene-like SiC sheet doped with palladium atom. We have selected a single graphene-like SiC layer, due to its more surface charge polarization in comparison with pure graphene which makes possible remarkable interactions with adsorbed hydrogen molecules. In our study we have included two different configurations of H_2 adsorption: 1) at the first state, hydrogen atoms after adsorption stretched and distance between H–H atoms has increased but their chemical bond doesn't break. In this situation a physical adsorption occurred and the binding energy restricts applicable interests where it is appropriate for reversible hydrogen storage; 2) at the second situation, atoms of hydrogen molecule discrete from each other and adsorption occurred in a chemical manner. As instance the when a H_2 molecule interact simultaneously with Pd atom and SiC nanosheet, it can be dissociated as in this case a hydrogen atom makes bond with Pd atom and the other can be adsorbed chemically on the SiC nanosheet surface. More details about adsorption mechanism are discussed it the context.

Introduction

Fuels based on hydrogen storage capability are systems that release very little environmental pollutants unlike fossil fuels. The use of hydrogen-based fuel cells needs solutions for the current challenges in the realm of technology. For instance we can point out to synthesize and design of the advance materials to reduce the costs of the hydrogen generation, transmission and maintenance [1]. Nanotechnology has introduced new materials with vast range of applications. Among them, carbon nanotubes, fullerenes, and graphene are extremely noteworthy. Recently, graphene-based materials included many significant researches, especially in the field of catalysis, electronics, optics and electro-chemical oxidation

* *Corresponding author.*
E-mail addresses: m.javan@gu.ac.ir, javan.masood@gmail.com (M. Bezi Javan).
http://dx.doi.org/10.1016/j.ijhydene.2016.09.081

and also hydrogen storage generation and production [1–4]. Experimental studies have shown that graphene-based materials can increase the hydrogen storage capacity up to 8.9 Wt. % [1–5]. In addition, practical usage of graphene has been discussed experimentally [6–14] and theoretically [15–18] as a purpose for generation and storage of energy in many articles. An appropriate idea to increase the adsorption of organic molecules on the surface of carbon nanostructures is based on doping their surface by metallic elements. So far, various investigations followed the use of this idea as a strategy for increasing the hydrogen molecule adsorption [19–21]. In fact the metal atoms have significant role to increase the binding energy of hydrogen molecules in a porous surface [22,23]. In a mechanism based on electrostatic interaction, the metallic atoms placed on surface of a nanostructure can bind multiple hydrogen atoms to itself [24–27]. Binding energy dependency of the hydrogen molecules to a transition metal was explained by the Kubas et al. [28]. Recent works have shown dramatic increase in hydrogen storage capacity in carbon nanotubes doped with Li and K atoms [19,20]. In an interesting work presented by Bath et al. [21] it has been observed an unusual adsorption of hydrogen molecules over porous carbons that chemically activated by alkali metals. However, many problems can be occurred for doping carbon nanostructures (for example graphene) with regards to the accumulation of doped atoms because the interactions between metallic atoms are rather stronger than molecules interactions such as hydrogen with carbons atom of graphene [29–31]. The influence of metallic impurities to the increment of the hydrogen adsorption is optimum when the impurities have maximum distance of each other which is conformable in the cases of small metallic nanoclusters. In recent work, the effect of small Pd clusters decorated on graphene was studied by Lopez et al. [32]. The reported results show that the Pd atoms can be bound to the graphene and provide the conditions for H_2 dissociation. However, according to the Lopez et al. [32] defects in graphene lattice can increase binding of the Pd atoms, as binding energy has increased almost 5 times in comparison with pure graphene. Overly, the literature reviews indicate the capacity of hydrogen storage in carbonic materials doped with Pd atoms is increased [33,34]. Choudhary et al. [35] theoretically studied the hydrogen storage on Cu and Pd-decorated graphene with single vacancy defect. They found that the single vacancy defect prevents the transition metal atom clustering and enables hydrogen molecule adsorption with higher value of binding energy. Zachariah et al. [36] reported 30% gain of hydrogen storage capacity of carbon nanotubes that doped with Pd atoms in room temperature and 1.67 *MPa* pressure in comparison with the pure carbonic nanotubes. In other interesting work Lipson et al. [37] showed that the thin layers of Pd confined in carbon nanotubes can increase the hydrogen storage capacity between 8 and 12 wt%. Other transition metals such as Pt and Ni have also been used in a similar way to increase hydrogen storage capacity in carbon based nanostructures [33–38]. In these cases the general mechanism of the surface activation is based on separated of hydrogen atoms over transition metal elements or clusters and in continue their overflow and adsorption over the carbon atoms surface [39]. In fact clusters of transition metal elements as primary sources of hydrogen in a catalytic process provided conditions for the adsorption of hydrogen atoms over activate carbon sites of the surface and are caused growth of the hydrogen adsorption.

A vast range of studies about hydrogen storage which have been reported theoretically confirm the increase in hydrogen storage capacity of carbon based nanostructures that doped with transition metals [25,27,40–46]. Such behaviors can be also seen in other nanostructure materials such as SiC nanotubes [47]. SiC nanotubes that were synthesized for the first time in 2001 [48] have a lot of potential application for use in high temperature, high power electronic and surface adsorption property due to great surface interactions [49–51]. The theoretical results show that the binding energy of H_2 to SiC nanotubes increased almost 20% compared to that of the pure carbon nanotubes according to rather ionic nature and also polarization of Si–C bonds [52]. These properties of SiC nanotubes (SiCNT) made them convenient for hydrogen storage. Special characters of SiCNT made them important in bonding with molecules such as H_2, CO_2, NO and etc., which rather weakly interacted with carbon nanotubes by van der Waals forces [53]. Especially the interactions between hydrogen and SiCNT have been the subject of several ab initio studies [54–57]. Zhao et al. [51] and Mpourmpakis et al. [52] have reported electronic characterization and structural properties of SiCNT at presence of the H_2 interaction. They found that a hydrogen storage capacity in SiCNT is 30% more than pure carbon nanotubes that consequently results to the introduction of SiCNT as new material for hydrogen storage. Another interesting work was performed by Gali [58] based on the total energy calculation of hydrogen adsorbed over SiCNT that doped with Boron, and Nitrogen atoms replaced in the lattice structure of nanotube. In addition, Wang et al. [59] in an ab initio study based on density functional theory (DFT) investigated interactions between H_2 molecules and doped Li atoms in SiC nanotubes. They found that a physical adsorption of hydrogen molecules on pure SiCNT with adsorption energy of about 0.086 eV, although the H_2 binding energy to Li atoms adsorbed on SiCNT is higher and reach to the value of 0.211 eV. A system containing Ti-doped graphene like SiC sheet and SiC nanotubes was studied by Banerjee et al. [60]. According to their work, an interacting hydrogen molecule with Ti ion on SiC sheet (or nanotube) leads to dissociation of the first hydrogen molecule in the atomic form and thereafter Ti atom adsorbs hydrogen in the molecular form. Also A similar study for Li and Ca doped graphene like SiC sheet has been investigated by Song et al. [61]. Barghi et al. [62] studied experimentally the hydrogen adsorption and desorption in SiC nanotubes. They found that the hydrogen storage capacity of the synthesized SiCNTs for the purified SiCNTs it is 50% higher than that of the corresponding carbon nanotubes. In our previous work, we investigated the hydrogen storage capacity of $Si_{60}C_{60}$ nano-cage based on a mechanism derived from density functional theory and molecular dynamics [47]. In this work, we investigate the adsorption of hydrogen in graphene-like SiC sheet doped with Pd atom. At first, preferred states of

Table 1 – Optimized geometry parameters and binding energy of the free H_2, PdH and PdH_2 systems.

Structure	Type	d_{Pd-H} (Å)	d_{H-H} (Å)	∠H-PD-H (θ)	E_b (eV)
H_2		–	0.748 (0.75,[a] 0.746[b])	–	−4.489 (−4.638,[a] −4.520[b])
Pd-H		1.56 (1.54,[a] 1.53[c])	–	–	−2.365 (2.630[a])
$Pd-H_2$	I	1.71 (1.69,[a] 1.68[d])	0.88 (0.90,[a] 0.88[d])	29.9 (31.0,[a] 30.4[d])	−0.884 (−0.936,[a] −0.837[d])
	II	1.77 (1.75,[a] 1.77[d])	0.80 (0.80,[a] 0.79[d])	2.3	−0.359 (−0.406,[a] −0.295[d])
	III	1.54 (1.54,[a] 1.52[d])	1.87 (1.76,[a] 1.74[d])	74.7 (69.8,[a] 69.8[d])	−0.743 (−0.761,[a] −0.642[d])
	IV	1.65 (1.66,[a] 1.64[d])	–	180.0	−0.091

[a] [25].
[b] [56,61].
[c] [57].
[d] [59].

hydrogen adsorbed and chemical bonds during the process of adsorption are explored. Then discussions about adsorption energy, energy band structures and density of states of desired structures are performed.

Computational details

The calculations were done based on density functional theory (DFT) by using OPENMX code which solves self consistently the Kohn–Sham equations. Crystal orbitals are expanded by using of a linear combination of numerical quasi atomic orbitals similar to method suggested by Sankey and Niklewski [63]. In all calculations LCAO basis set used for ground state simulation of the systems and calculation of the Bloch wave functions. For creating exact description of the charge density in real space and self-consistent calculation of the Hamiltonian matrix, a cut off limitation about 150 Ry was determined for integration. Ionic nucleus interactions were considered in the framework of norm-conserving fully separable Troullier–Martines pseudopotential [64] in Kleinman–Bylander [65] aspect in our calculations. Binding energy for an atom or adsorbed molecule (X) can be determined as the following equation:

$$E_b(SiC + X) = E_T(SiC + X) - [E_T(SiC) + E_T(X)] + \Delta_{BSSE} \quad (1)$$

where $E_T(SiC)$ total energy of a pure SiC sheet, $E_T(X)$ is total energy of an isolated of X atom or molecule and also $E_T(SiC + X)$ is total energy of functionalized SiC sheet with X atom or molecule. Negative values of the binding energy indicate the exothermic adsorption. In this work we used spin polarized generalized gradient approximation (GGA) as parameterized by Perdue et al. (PBE) [66]. The Δ_{BSSE} added for correcting the superposition errors of the ground state basis sets as they are used for description of the interacting systems [67]. To ensure removing extra interactions between SiC sheets in neighbor supercells we have considered a vacuum region about 25 Å in all calculations because at this amount of distance between two unit cells, we have a minimal change in total energy of the systems. All atoms have been relaxed in the extended region. Inter atomic forces calculated based on Hellmann–Feynman force calculation method [68] and the structures were optimized based on conjugated gradient approximation [69]. The systems were optimized at room temperature while the mean square of the obtained forces reaches to less than or equal to 0.05 eV/Å.

In order to estimate the accuracy of the calculations, we first studied the fcc bulk structure of Pd lattice with Mokhorst-Pack K-point 8 × 8 × 8. In optimization process, the lattice constant obtained about 3.86 eV/Å, in addition a cohesive energy was calculated to be 3.75 eV/Å, which is in agreement with the experimental results (3.86 eV/Å) [70]. Also we studied bond lengths and dissociation energy of the H_2, PdH and PdH_2 molecules which are compared with the results of the previous works shown in Table 1. According to Table 1, the results are in good agreement with previously reported experimental and theoretical studies [71–73].

At first we consider a Pd atom on a SiC sheet. One Pd atom per unit cell was considered at different sites with high symmetry. Valuable high symmetry positions are: the top sites on the carbon and silicon, hollow sites on the hexagonal rings center and bridge sites on the middle of Si–C bonds (as shown in Fig. 1). Based on Lopez et al. [32] we present several structural parameters for the adsorption sites of the Pd after structural optimization: z_{SiC-Pd} is defined as vertical distance from the Pd atom and mean z coordinates of the Si and C atoms of SiC sheet, $d_{Si,C-Pd}$ is average distance between Pd atom and nearest silicon or carbon atom, Δz is defined as a parameter estimating the

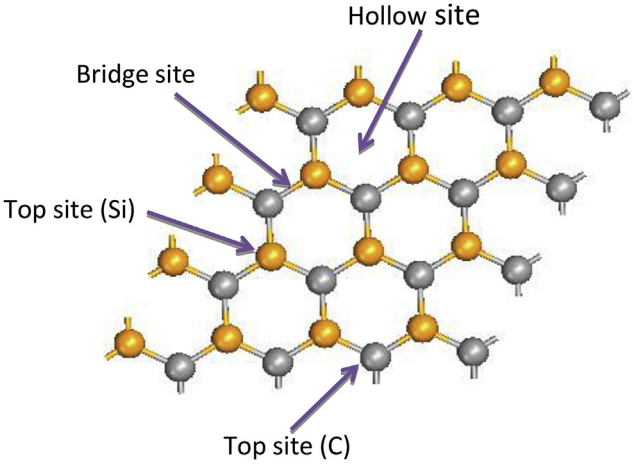

Fig. 1 – Schematic representation of the SiC sheet unit cell. The four adsorption sites are shown as hollow, bridge, top site (Si) and top site (C).

deviation of the SiC plane along Z-axis direction. The binding energy of Pd atoms to the SiC sheet can be estimated as the following formula:

$$E_b(Pd) = E_T(SiC/Pd) - [E_T(Pd) + E_T(SiC)] \quad (2)$$

where $E_T(SiC)$ total energy of a pure SiC sheet, $E_T(Pd)$ is total energy of an isolated of Pd atom and also $E_T(SiC/Pd)$ is total energy of functionalized SiC sheet with Pd atom. A negative value of binding energy describes an attractive interaction. In similar way, according to Lopez et al. [32], in the following we study the adsorption of hydrogen atom and molecule on the SiC sheet that doped with Pd atom by considering different positions of PdH (PdH_2) as shown in Fig. 2. The side and end-on interaction of H_2 with Pd atoms was considered during the formation of PdH_2 systems [74,75]. So in primary calculation we study the interaction between hydrogen atom and Pd atom adsorbed on SiC sheet. We obtain optimal distance of Pd-H by determining the different positions of the hydrogen atom during interaction with Pd located at situations that already mentioned on SiC sheet as shown in Fig. 2. According to the configurations presented by Lopez et al. [32] then we study the adsorption of a dihydrogen molecule on Pd doped SiC sheet with considering different positions of PdH_2 as are labeled from **I** to **IV**. In fact both side-on and end-on adsorption is considered in the binding energy calculations.

The **I** and **II** structures refer to the side-on and end-on configurations as the H–H bond remain stable after relaxation while in the side-on of the **III** and **IV** structures H–H bond is broken, which is in agreement with Lopez et al. [32]. In the study of these structures H–H and Pd–H bond length (d_{H-H}, d_{Pd-H}) and angle between H-Pd-H ($\angle$H-Pd-H) determined for free and adsorbed systems. The structural parameters such as vertical distance of Pd atom from SiC sheet (Z_{SiC-Pd}), average distance of the Pd atom from Si or C atom of the SiC sheet ($d_{Si,C-Pd}$) and deviation of the SiC sheet along z axis (Δz) assessed during adsorption on SiC sheet. We also obtained the rotation angle of the hydrogen molecules towards substrate (see θ in Fig. 2). The adsorption energy of the H_2 on the Pd doped SiC sheet can be obtained as follows:

$$E_b(H_n) = E_T(SiC/Pd/H_n) - [E_T(SiC/Pd) + E_T(H_n)] \quad (3)$$

n is equal to 1 or 2 according to the number of H atoms, $E_T(Pd/SiC)$ denotes to the total energy of functionalized sheet with Pd, $E_T(H_n)$ is total energy of H and H_2 structures and $E_T(H_n/Pd/SiC)$ is total energy of Pd doped SiC sheet with

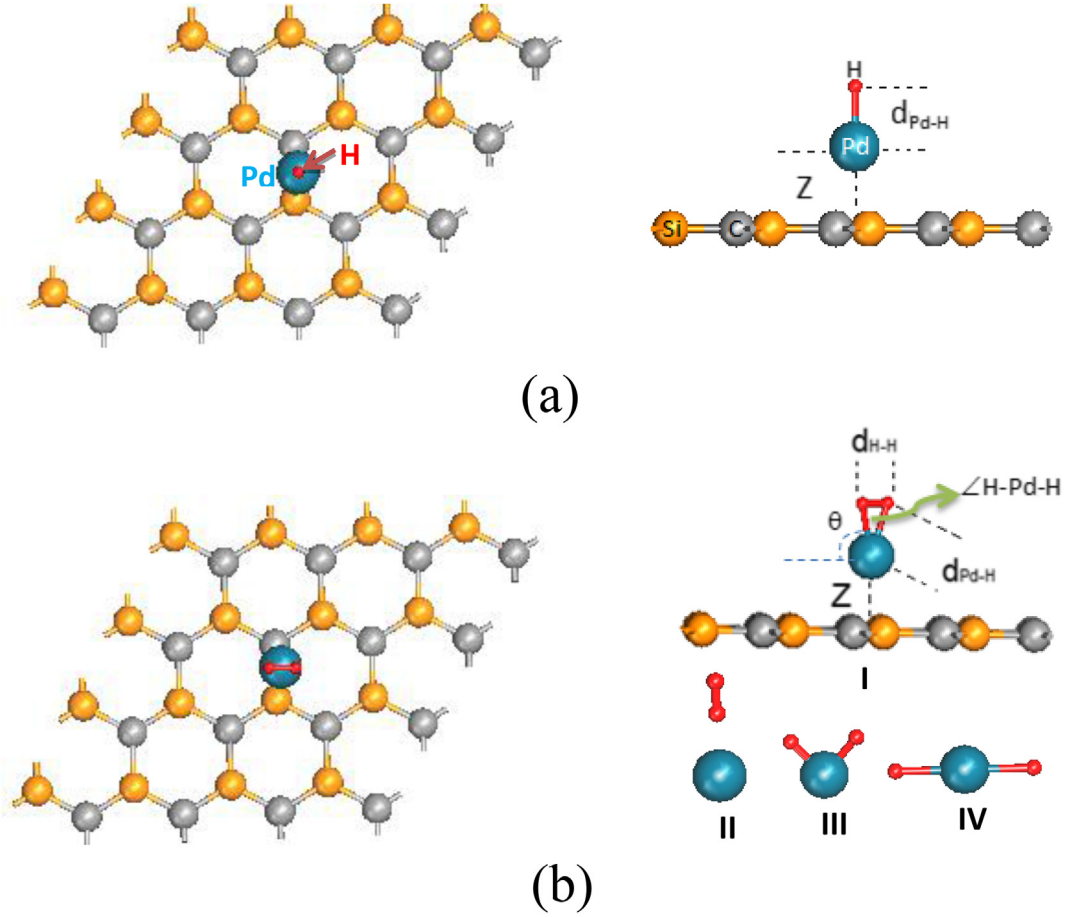

Fig. 2 – Geometry structures of the: (a) SiC/Pd/H and (b) SiC/Pd/H_2 systems.

adsorbed hydrogen atom or molecules. Study of the electronic properties and chemical bonding of the adsorbed H or H_2 molecule is possible with analysis of the density of states (DOS), band structure and also crystal orbital overlap population (COOP) of the considered systems.

Results and discussion

Adsorption positions

Optimized structures for the free PdH, PdH_2 and SiC supported systems were studied and results are listed in Tables 1 and 2. The interaction between the H_2 molecules and Pd atoms is well-known, so to check the accuracy of our calculations the obtained results compared with earlier works and presented in Table 1. In order to compare results of the SiC/Pd system with similar systems based on graphene, the results obtained with **I** to **IV** configurations were compared with Lopez et al. [32]. According to the data presented in Table 1, the binding energy of a hydrogen molecule is about −4.49 eV which is in agreement with previous studies [71,76]. Also the H–H bond length for free H_2 molecule is 0.748 Å which is close to the data presented by Lopez et al. [32] and Weast et al. [71]. The binding energy of PdH molecule decreased to −2.36 eV owing to the weaker interaction between Pd-H than H-H coupling. Reducing the binding energy value of PdH molecule is associated with elongation of Pd–H bond length (1.56 Å) than H–H bond length (0.748 Å) in H_2 molecule. These results are in agreement with previous GGA-DFT calculation.

The interaction between H_2 molecules with an isolated Pd atom can lead to the further reduction of the binding energy and elongation of the Pd–H bond length in some manners. As it can be clearly seen from Table 1, from **I** to **IV** configurations of H_2-Pd interaction, the highest value of the binding energy is related to **I** system that called the Kubas complex, as hydrogen molecules don't break and H–H bond remains stable where the H_2 molecule locates exactly on Pd atom in horizontal shape. The obtained results have also a good agreement with Lopez et al. [32]. In Kubas state the binding energy of the PdH_2 system is about −0.884 eV which is significantly lower than H_2 or PdH systems. The secondary most stable state is related to **III** configuration as in this state two H atoms are attached to the Pd atom with optimized ∠H-Pd-H angle of 74.75°. In this state the calculated binding energy is about 0.141 eV less than of Kubas state.

We have also two linear PdH_2 system indexed as **II** and **IV**. The **II** configuration is end-on approaching mode, as H_2 binding energy is about −0.359 eV which is lower than **I** and **III** configurations. In this case the optimized structure of H_2 molecule slightly turn to the SiC sheet as it is not perfectly vertical on the Pd atom so makes a little angle of ∠H-Pd-H just

Table 2 – Optimized geometry parameters and binding energy and energy band gap of the SiC/Pd, SiC/Pd/H and SiC/Pd/H_2 systems. All distances are presented in Å.

System		Site	Z_{SiC-Pd}	$d_{Si,C-Pd}$	d_{Pd-H}	d_{H-H}	∠H-Pd-H	(θ)	E_b (eV)	E_g
SiC/Pd										
		Top-C	2.16	2.56, 2.16	–	–	–	–	−1.91	1.82
		Top-Si	2.27	2.27, 2.96	–	–	–	–	−1.89	1.61
		Bridge	1.92	2.52, 2.17	–	–	–	–	−2.53	2.05
		Hollow	1.81	2.52, 2.62	–	–	–	–	−2.51	2.03
SiC/Pd/H										
		Top-C	2.23	2.63, 2.30	1.65	–	–	90	−2.95	2.55 (2.45)[a]
		Top-Si	2.20	2.27, 2.47	1.62	–	–	82.8	−2.81	2.01 (1.41)[a]
		Bridge	2.30	2.45, 2.70	1.63	–	–	82.78	−3.01	2.45 (2.36)[a]
		Hollow	1.99	2.49, 2.52	1.61	–	–	51.32	−2.99	2.42 (2.41)[a]
SiC/Pd/H_2										
	I	Top-C	1.98	2.59, 2.15	1.79	0.82	26.42	75.04	−3.14	2.32
		Top-Si	2.00	2.56, 2.64	1.79	0.81	25.90	73.90	−2.01	1.82
		Bridge	2.34	2.15, 2.60	1.80	0.82	26.40	71.30	−3.18	2.36
		Hollow	1.87	2.66, 2.72	1.80	0.84	27.05	65.68	−3.17	2.30
	II	Top-C	2.15	2.65, 2.15	1.98	0.76	0.93	89.42	−2.79	2.19
		Top-Si	2.19	2.19, 2.62	2.10	0.76	18.51	66.02	−2.79	2.36
		Bridge	2.37	2.65, 2.15	1.81	0.82	25.80	82.24	−2.01	2.31
		Hollow	1.90	2.71, 2.40	1.85	0.84	26.69	60.34	- 2.77	2.35
	III	Top-C	2.16	2.60, 2.16	1.79	0.82	26.10	64.53	−2.51	
		Top-Si	2.16	2.34, 2.56	1.86	0.80	25.10	64.08	−2.48	
		Bridge	2.18	2.56, 2.34	2.22	0.76	14.89	48.56	−2.75	2.58
		Hollow	2.02	2.55, 2.34	1.58	1.63	61.52	45.63	−2.46	2.48
	IV	Top-C	2.10	2.80, 2.10	1.59	–	176.67	4.33	−2.01	1.00
		Top-Si	2.14	2.54, 2.14	1.57	–	170.21	9.36	−1.65	1.65
		Bridge	2.10	2.68, 2.11	1.56	–	174.94	6.06	−2.02	1.04
		Hollow	2.14	2.57, 2.14	1.82	0.804	26.68	62.75	−2.01	0.89

[a] For SiC/Pd/H system the Eg data are separated for up and down spin states. The data in parentheses show that the band gap for down spin states.

2.3°. The **IV** configuration has binding energy about −0.091 eV although here we obtained this structure stable (due to its negative binding energy) but this structure reported unstable in Lopez et al. [32]. Generally the obtained results in Table 1 are in agreement with previous works [32,74] as the binding energy of H_2 molecule to the Pd atom can be ordered as E_b(I) > E_b(III) > E_b(II) > E_b(IV).

In continue, we performed the first study of the SiC/Pd system as a subsystem for interacting with H atom or H_2 molecules. The four different situations of top-C, top-Si, hollow and bridge sites (see Fig. 1) of the SiC sheet are examined for Pd atom adsorption. Regarding to the surface properties of SiC sheet doped with Pd atoms, it can be found from Table 2 that the most stable position for a Pd atom is a bridge site of the SiC sheet. Although the binding energy on top-C, Si and hollow sites are very close to the bridge state with differences about 0.62 eV–0.64 and 0.02 eV, respectively. The weakest binding energy occurs on top-Si position. The vertical distance of the Pd atom from SiC sheet (Z_{SiC-Pd}) represents that the Pd atom gets closer distance from SiC sheet in bridge and hollow sites than the top site of related states. Deformation of the SiC sheet along the axis perpendicular to the surface (Δz) is between 0.13 and 0.34 Å. Similar calculations by Chan et al. [77] and also Lopez et al. [32] indicate to Δz < 0.1 Å for graphene.

Comparing Pd binding energy to the SiC sheet indicate that it is almost 2.32 times more than binding energy on graphene. The recent GGA-DFT calculations presented by Maiti and Rica [78] indicate that stable position for adsorptions of Pd atoms on a monolayer graphene is in top site position. This result somewhat different in case of carbon nanotubes as the DFT calculations presented by Durgun et al. [79] and Xiao et al. [43] show that bridge states on C–C bonds parallel to the axis of carbon nanotubes (CNTs) are suitable for adsorbing Pd atom and has higher value of the binding energy as it is about 0.66 eV where the C–Pd bond length is about 2.12 Å. According to Mitta and Rica [78] results, binding energy of Pd to the graphene is about 4% less than its binding energy to the CNTs due to the curvature of the CNT structures which caused stronger interactions between nanotube and Pd atom. According to the Lopez et al. [32] finding the binding energy of Pd on graphene changed between 0.897 and 1.077 eV for different situation of doping which is less than binding energy of Pd to the SiC sheet.

We have been considered the SiC/Pd/H system for analysis. Regarding to the binding energy of the H atom to the SiC/Pd system which is described in Table 2, it can be clearly seen, the SiC/Pd in bridge site configuration in a preferential position for the adsorption of H atoms on Pd atom. In this case the binding energy of the H atom to the SiC/Pd system is about −4.08 eV which shows the stable state due to the negative binding energy value. Although the binding energy for different configurations has small differences about 0.02–0.07 eV with most stable states as the H atom has lowest binding energy to the SiC/Pd system in top-Si configuration. Comprising the binding energy of the H to the SiC/Pd system with binding energy of the H to the isolated Pd atom (see Table 1) show that the binding energy of the H atom has a significant increment about 1.6 eV. The gain of the H binding energy can be related to the electrostatic interaction between H and Pd atoms as charge polarization of Pd increased after locating on SiC sheet. In the case of SiC/Pd system the interaction between H and SiC sheet is not very significant regarding to the H atom which is approximately located in vertical states ($51.32 \leq \theta \leq 90$) sufficiently far from SiC sheet. On the other hand, the Pd-H interaction increases the distance of the Pd from SiC sheet as it can be seen from Z_{SiC-Pd} presented in Table 2. In all considered cases deformation of SiC layer along z axis is Δz < 0.44 Å.

However, in the case of SiC/Pd/H system, the DFT calculations are not available, but similar calculations for H adsorption on Pd doped graphene is exist based on Lopez et al. [32]. The most stable position for adsorption of the H atom is on Pd directly located on Si–C bond of the SiC sheet as we name this state as bridge site. However in this case the Pd atom somewhat is moved to the carbon atoms. The Pd–H bond length in isolated molecular structure is slightly shorter than Pd–H bond length when it is placed on the SiC sheet due

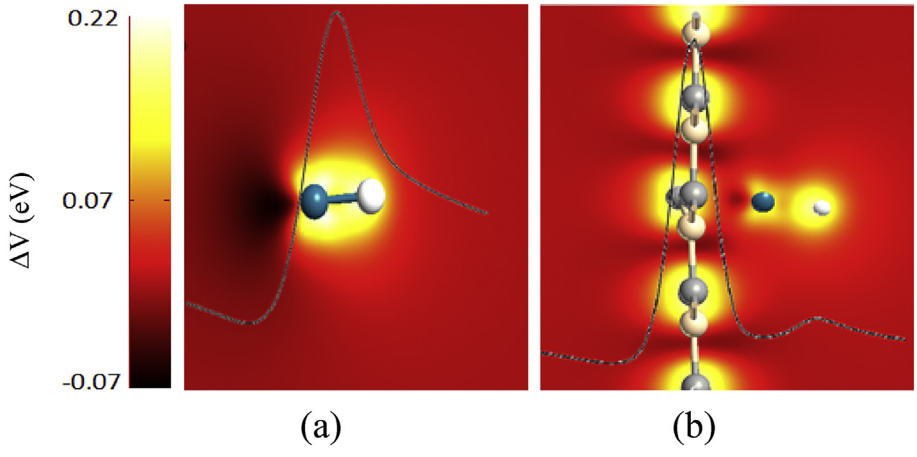

Fig. 3 – The contour plot of the electrostatic difference potential (ΔV (eV)) for a) PdH and b) SiC/Pd/H systems. The light and dark regions show the location of the charge accumulation and depletion, respectively. The curve inside the figure shows the average electrostatic optional around PdH molecule.

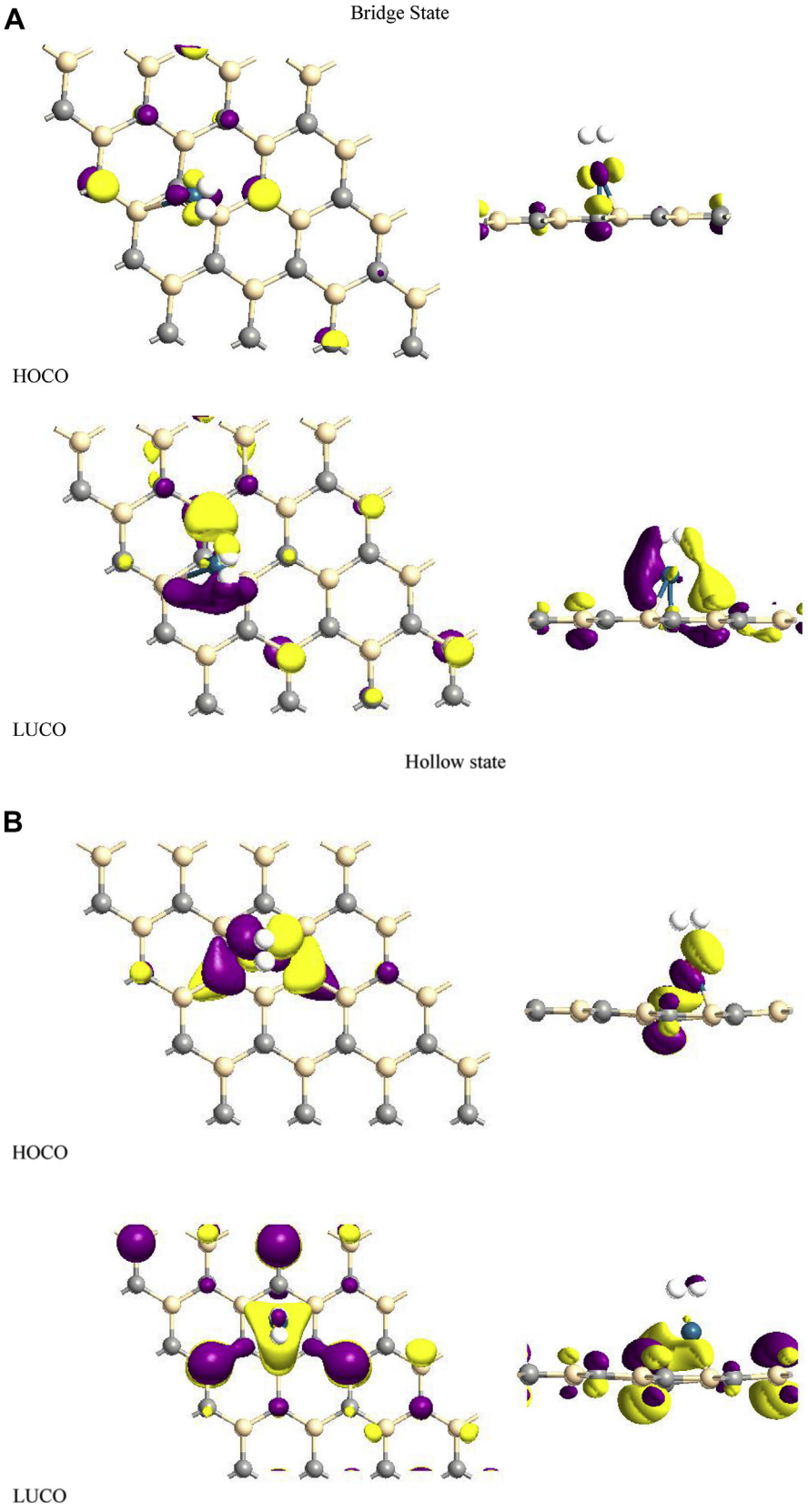

Fig. 4 – Highest occupied (HOCO) and lowest unoccupied (LUCO) crystal orbitals of the most stable configurations of (I)-SiC/Pd/H_2 system for (a) bridge and (b) hollow states from top and side views.

to interaction between Pd and H atoms in SiC/Pd/H structure, similar to the graphene case [32]. In all structures of SiC/Pd/H, bond length of Pd–H is in the range of 1.61–1.64 Å. For examined configurations the binding energy of the H atom to the SiC/Pd substrate is ~−3 eV which is significantly larger than the binding energy of the H atom to the isolated Pd atom (~−2.3 eV). Also the binding energy of the H atom to the graphene/Pd substate is ~2.9 eV for bridge state as it is slightly larger than the binding energy than the isolated Pd atom [32]. Based results, it can be concluded that H atom can bind to the SiC/Pd substrate with energy larger than graphene/Pd or isolated Pd systems (near 0.2 eV difference). This behavior can be originated from the induced electrostatic potential to the SiC sheet after doping one Pd atom. In Fig. 3, it has depicted a contour plot of the electrostatic difference potential around isolated PdH molecule and SiC/Pd/H system. The dark and light regions show the location of the negative and positive charges concentration. It can be seen from figure that, the negative charge around Pd atom has increased due to charge polarization of the SiC sheet as the quantum well behind H atom is deeper in comparison with free PdH molecule about 0.15 eV.

Finally we study the adsorption of H_2 molecules on SiC sheet that functionalized by Pd atom. With regard to the binding energy that presented in Table 2, the most stable state of SiC/Pd/H_2 is belonged to the Kubas structures that named **I** as the structural parameters of top-c, bridge and hollow sites of doping are almost very close to each other. In comparison with SiC/Pd/H system the binding energy of the H_2 molecule to the SiC/Pd substrate has a little growth in contrast to the graphene based system [32]. According to the Lopez et al. [32] the binding energy of the H_2 molecule to the graphene/Pd substrate is ~1.1–1.9 eV for various configurations of H_2 adsorption states. This condition is the results of the higher charge polarizability of the SiC sheet than graphene due to the Pd decoration. The corresponding states for highest occupied and lowest unoccupied crystal orbitals (HOCO and LUCO) for bridge and hollow states which have higher stability in Kubas configurations are shown in Fig. 4. The light and dark parts show the positive and negative sign of the wave functions. The concentration of the wave function shows the active sites of the system at the equilibrium state. As it can be observed, the in HOCO of the bridge and hollow states the active sites mainly concentrated on SiC/Pd substrate but the LUCO somewhat is made from H atomic orbitals hybridization with SiC/Pd crystal orbitals.

The H_2 binding energy in **II** configurations of SiC/Pd system is somewhat close to the **III** configurations but small deviations in order of 0.2 eV are made. The optimized structures show that the hydrogen molecules in this state turn to the Kubas state and their positions shift to the bridge or top-C sites. The bond length of the adsorbed H_2 molecule on SiC/Pd sheet is increased from 0.76 to 0.819 Å. Also In hollow state of **III** configuration, the distance between hydrogen atoms is equal to 1.63 Å that means the H–H bond is ruptured. In general, the same result about the graphene/Pd/H_2 and single walled carbon nanotube (SWCNT)/Pd/H_2 has been reported [32,43].

In the case of **IV** states, the binding energies of all examined positions were significantly less than that of **I** to **III** binding energies discussed above. In contrast to the graphene/Pd/H_2 system or carbon nanotubes, dissociation of hydrogen molecules is not observed in these cases -H bond is broken and one H atom is adsorbed on the surface of SiC and the second H atom make bond to the Pd atom. Although in all cases, the Pd atom moves to the top-C state after optimization. In Fig. 5, it has shown that the H_2 molecule is dissociated on top-C state of the SiC/Pd/H_2 system for **IV** optimized configuration. In fact in this situation, atoms of hydrogen molecule discrete from each other and adsorption occurred in a chemical manner.

According to the values of Table 2, a general behavior can be seen, as the binding energy of different states in top-C is more than binding energy in top-Si, also the binding energy of bridge states are more than the hollow states. In all cases, the distortion of SiC layer is very low when interacting with Pd atom and H_2 molecule and rotation of hydrogen molecules along the z-axis (θ) has a little impact on binding energy. In

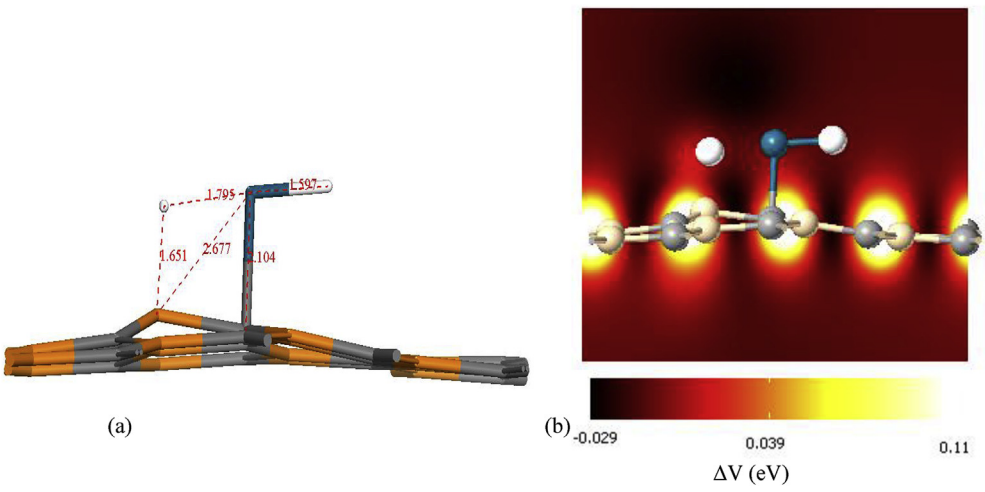

Fig. 5 – (a) The optimize geometry and structural parameters of SiC/Pd/H in bridge state, (b) the contour plot of the electrostatic difference potential (ΔV (eV)) of the corresponding bridge SiC/Pd/H_2 system.

comparison with isolated states, the binding energy of H_2 molecules to SiC/Pd structure was meaningfully increased and this growth is more than things reported for graphene and CNTs, therefore the results indicate that the SiC sheets that covered by Pd atoms can provide convenient stability for better adsorption of H_2 molecules.

Analysis of chemical bonding and electronic properties

To compare the obtained results with earlier theoretical works on graphene, we studied the chemical bonds during the H or H_2 adsorption on SiC/Pd substrate according to the analysis of crystal orbital overlap population (COOP) belonging to the pair atoms (C-Pd, Si-Pd and H-Pd) that provided preferred positions for adsorptions. These states are bridge configurations for SiC/Pd/H and Kubas complex of SiC/Pd/H_2 which refer to the most stable structures from binding energy point of view. The COOP curves for C-Pd, Si-Pd and H-Pd in the process of adsorption of H and H_2 on the single layer of SiC/Pd structure are shown in Fig. 6. Positive and negative parts of COOP show "bonding" and "anti-bonding" states, respectively.

Regarding to the most stable adsorption position of Pd on bridge state, COOP curves of Pd-H, Pd-C and Pd-Si show a distribution of bonding and anti-bonding states near the Fermi level in all configurations including with or without H or H_2 adsorbents. The same behavior for graphene/Pd/H(H_2) systems have been reported by Lopez et al. [32]. Both SiC/Pd/H(H_2) systems have significant bonding states close to −5 eV

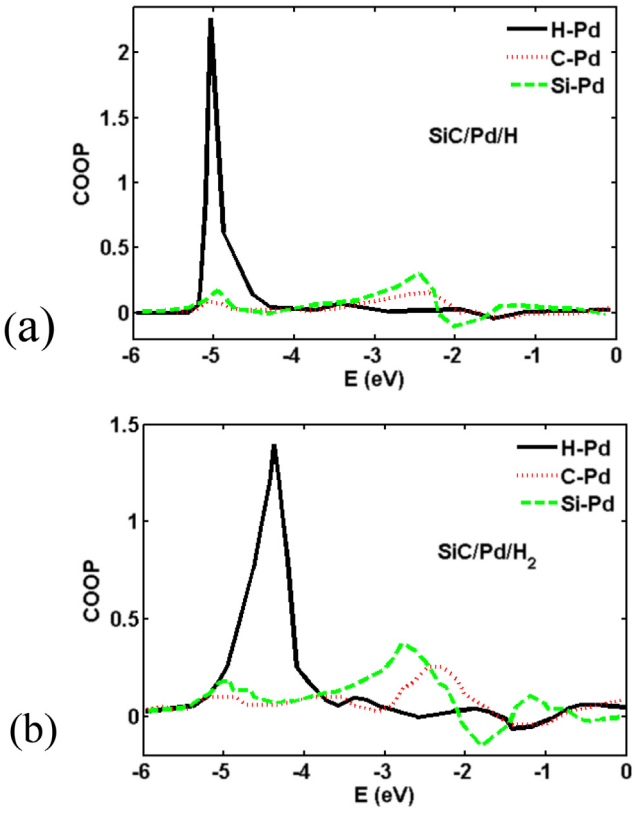

Fig. 6 – COOP curves for H-Pd, Si-Pd and C-Pd bonds in the most stable structures of the (a) SiC/Pd/H and (b) SiC/Pd/H_2 systems.

which indicate the H-Pd strong coupling. The value of the COOP for SiC/Pd/H is higher than corresponding systems for SiC/Pd/H_2 which means more overlap of the H and Pd atoms. This refers to the higher values of binding energy of the single hydrogen atom to the Pd/SiC system which is in agreement with data presented in Table 2. For SiC/Pd/H_2 some bonding and anti-bonding states raise near Fermi level (E = 0) as we can see that the C-Pd and Si-Pd interaction make a bonding and antibonding states, respectively.

In Fig. 7 density of states (DOS) curve of the pure SiC, SiC/Pd, SiC/Pd/H and SiC/Pd/H_2 systems in their most stable configurations are shown. In all DOS curves the contribution of the electronic states have been projected on included atoms (Si, C, Pd and H atoms). The band gap of the SiC nanosheet is about 3.7 eV as the energy gap of the Pd doped systems has significant changes according to the different configuration of doping. Also we can see different values of energy gap (E_g) for SiC/Pd/H and SiC/Pd/H_2 according to the data presented in Table 2. Regarding to the E_g of the considered system in their most stable configuration we can find the energy gap are 2.05, 2.36 (down spin state) and 2.36 eV for SiC/Pd, SiC/Pd/H and SiC/Pd/H_2 system, respectively. In fact a new donor states appear inside the gap which can be seen clearly in band structure plotted in Fig. 8.

The scheme of SiC/Pd/H and SiC/Pd/H_2 is somewhat different from band structure point of view. In comparison with pure SiC and SiC/Pd band structures we can see a partial spin splitting in the valence and conduction bands as the valence band edge of the SiC/Pd system is strongly affected by new electronic states. The spin polarized DFT calculations indicate that the new states inside gap are fully spin polarized as a level of acceptor type with spin down state appear at the edge of the valence band. This band state is created by hybridization of Pd-4d and H-1s orbitals. The Mulliken population analysis, electronic charge and spin for various configurations are shown in Table 3. According to data presented in table, it can be clearly observed that the H atom in SiC/Pd/H system has net charge just −0.103 and −0.098e for bridge and top-C states, respectively. On the other hands, the corresponding charges on Pd atom in bridge and hollow sites are −0.414 and −0.386 e, respectively. In the case of the SiC/Pd/H_2 systems the charge on each H atoms has a positive sign as its value is +0.05e for both bridge and top states. Regarding to this results, it can be concluded that, the electrostatic interaction between H and Pd is the main reason for higher binding energy values in SiC/Pd/H_2 than the SiC/Pd/H because in both of them, Pd atom has negative net charge while the H atoms have positive value of charge in SiC/Pd/H_2 in contrast of SiC/Pd/H system.

According to the values in Table 3, for SiC/Pd/H system the induced spin moment on Pd and H atom are 0.551 and 0.273μ_B, respectively. Such behavior of magnetization can be a distinguishing feature of SiC/Pd/H from SiC/Pd/H_2. For SiC/Pd/H_2 system the conduction band edge degeneracy split due to the H_2 interaction with SiC/Pd system and narrow sub-band appears in the gap of the SiC sheet. According to the figure the valence band of the SiC/Pd and SiC/Pd/H_2 systems are very similar without any spin polarization in electronic states.

In brief, we have found the catalytic activity of the Pd atom located on the SiC nanosheet as a substrate. We found that the

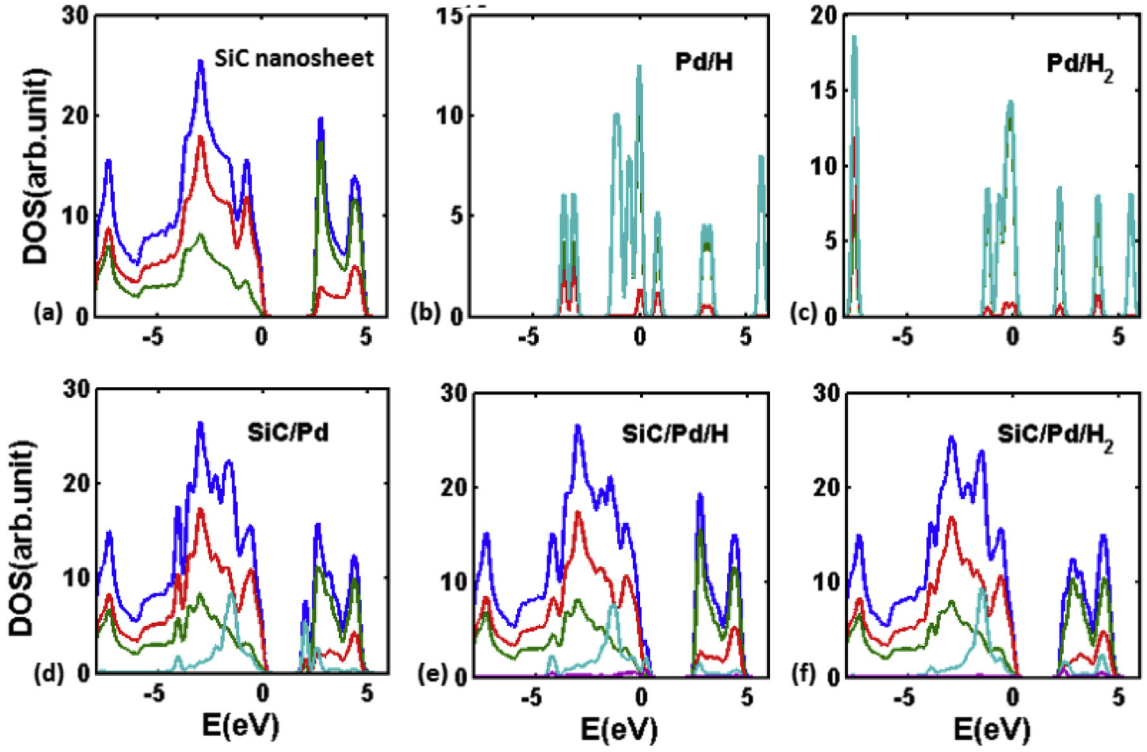

Fig. 7 – Total and projected density of states of the palladium (Pd) doped silicon carbide (SiC) nanosheet: (a) pure SiC nanosheet, (b) isolated PdH, (c) PdH_2 molecules and (d) SiC/Pd, (e) SiC/Pd/H and (f) SiC/Pd/H_2 systems.

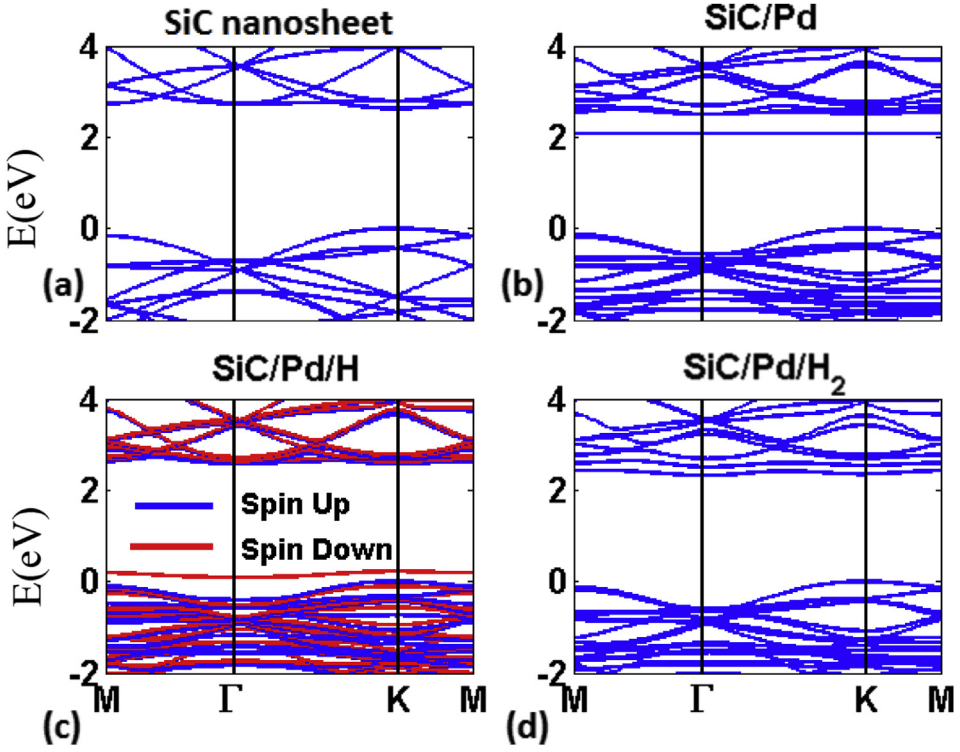

Fig. 8 – Band structure of the most stable configurations of the pure (a) SiC nanosheet, (b) SiC/Pd, (c) SiC/Pd/H and (d) SiC/Pd/H_2 systems.

Table 3 – Mulliken charge (spin) population of the most stable configurations for considered complexes.

System	Site	C			Si			Pd				H		
				Q/e			Q/e				Q/e			Q/e
Orbitals		2s	2p		3s	3p		5s	5P	4d		1s		
SiC/Pd	Hollow	1.667	3.511	−1.178	0.881	1.438	1.681	0.771	0.315	9.364	−0.449			
	Bridge	1.675	3.51	−1.185	0.859	1.389	1.752	0.761	0.302	9.351	−0.413			
SiC/Pd/H	Hollow	1.633 (−0.003)	3.59 (−0.016)	−1.223 (−0.016)	0.867 (0.001)	1.41 (−0.006)	1.723 (−0.007)	0.89 (0.338)	0.30 (−0.017)	9.187 (0.249)	−0.386 (0.569)	1.10		−0.098 (0.236)
	Bridge	1.639 (−0.818)	3.575 (−1.780)	−1.214 (0)	1.406 (−0.008)	1.406 (−0.008)	1.188	0.873 (0.325)	0.337 (−0.013)	9.175 (0.239)	(0.551) −0.414	1.103	(0.273)	−0.103
SiC/Pd/H_2														
I	Hollow	1.64	3.608	−1.248	0.85	1.422	1.728	0.936	0.265	9.338	−0.538	0.95	0.05	
II	Bridge	1.64	3.948	−1.488	0.85	1.368	1.782	0.936	0.265	9.338	−0.539	0.95	0.05	

Q = total charge.
*For SiC/Pd/H systems the net spin moments are shown in parenthesis.

hydrogen atom as well as H_2 molecule can bin to the Pd atom in a chemisorption process as in some situations we can see H_2 dissociation. According to our results some H or H_2 interacting configurations with SiC/Pd subsystem have higher value of binding energy and so higher structural stability.

Conclusion

Graphene-like SiC sheet decorated with Pd atom was investigated as a promising material for hydrogen storage or H_2 dissociation. A theoretical approach based on density functional theory (DFT) was applied to study of the interaction between hydrogen molecule and a graphene-like SiC sheet doped with Pd atom. In our study we have included two different configuration of H_2 adsorption: 1) At the first state, hydrogen atoms after adsorption stretched and distance between H–H atoms has increased but their chemical bond doesn't break. In this situation a physical adsorption occurred and the binding energy restricts applicable interests where it is appropriate for reversible hydrogen storage; 2) At the second situation, atoms of hydrogen molecule discrete from each other and adsorption occurred in a chemical manner. The distortion of SiC layer is very low when interacting with Pd atom and H_2 molecule and the rotation of hydrogen molecules along the z-axis (θ) has a little impact on binding energy. In comparison with a free state, the binding energy of H_2 molecules to SiC/Pd structure was meaningfully increased and this growth is more than things reported for graphene and carbon nanotubes based systems. Therefore, the results indicate that the SiC sheets that covered by Pd atoms can provide convenient stability for better adsorption of H_2 molecules.

REFERENCES

[1] Tozzini V, Pellegrini V. Graphene, related two-dimensional crystals, and hybrid systems for energy conversion and storage. J Phys Chem C 2011;115:25523.

[2] Liu CJ, Burghaus U, Besenbacher F, Wang ZL. Preparation and characterization of nanomaterials for sustainable energy production. ACS Nano 2010;4:5517.

[3] Yang JH, Mu D, Gao YJ, Tan J, Lu AH, Ma D. Cobalt phthalocyanine–graphene complex for electro-catalytic oxidation of dopamine. J Nat Gas Chem 2012;21:265.

[4] Wang N, Wang L, Tan Q, Pan YX. Effects of hydroxyl group on H_2 dissociation on graphene: a density functional theory study. J Energy Chem 2013;22(3):493–7.

[5] U. S. DOE, http://www.eere.energy.gov/hydrogenandfuelcells/mypp/ [Accessed 15 July 2011].

[6] Li YG, Wang HL, Xie LM, Liang YY, Hong GS, Dai HJ. MoS_2 nanoparticles grown on graphene: an advanced catalyst for the hydrogen evolution reaction. J Am Chem Soc 2011;133(19):7296–9.

[7] Qian Z, Hudson MSL, Raghubanshi H, Scheicher RH, Pathak B, Araujo CM, et al. Excellent catalytic effects of graphene nanofibers on hydrogen release of sodium alanate. J Phys Chem C 2012;116(20):10861–6.

[8] Parambhath VB, Nagar R, Ramaprabhu S. Effect of nitrogen doping on hydrogen storage capacity of palladium decorated graphene. Langmuir 2012;28(20):7826–33.

[9] Wang Y, Liu JH, Wang KA, Chen T, Tan X, Li CM. Hydrogen storage in Ni–B nanoalloy-doped 2D graphene. Int J Hydrogen Energy 2011;36(20):12950–4.
[10] Lv XJ, Fu WF, Chang HX, Zhang H, Cheng JS, Zhang GJ, et al. Hydrogen evolution from water using semiconductor nanoparticle/grapheme composite photocatalysts without noble metals. J Mater Chem 2012;22(4):1539–46.
[11] Cheng P, Yang Z, Wang H, Cheng W, Chen MX, Shangguan WF, et al. TiO_2–graphene nanocomposites for photocatalytic hydrogen production from splitting water. Int J Hydrogen Energy 2012;37(3):2224–30.
[12] Ma LP, Wu ZS, Li J, Wu ED, Ren WC, Cheng HM. Hydrogen adsorption behavior of graphene above critical temperature. Int J Hydrogen Energy 2009;34(5):2329–32.
[13] Darkrim FL, Malbrunot P, Tartaglia GP. Review of hydrogen storage by adsorption in carbon nanotubes. Int J Hydrogen Energy 2002;27(2):193–202.
[14] Züttel A, Sudan P, Mauron P, Kiyobayashi T, Emmenegger C, Schlapbach L. Hydrogen storage in carbon nanostructures. Int J Hydrogen Energy 2002;27(2):203–12.
[15] Zhou Z, Zhao J, Chen Z, Gao X, Yan T, Wen B, et al. Comparative study of hydrogen adsorption on carbon and BN nanotubes. J Phys Chem B 2006;110(27):13363–9.
[16] Takahashi K, Isobe S, Omori K, Mashoff T, Convertino D, Miseikis V, et al. Revealing the multibonding state between hydrogen and graphene-supported Ti clusters. J Phys Chem C 2016;120(24):12974–9.
[17] Li J, Zhao Y, Tan HS, Guo Y, Di CA, Yu G, et al. A stable solution-processed polymer semiconductor with record high-mobility for printed transistors. Sci Rep 2012;2:754.
[18] Park HL, Chung YC. Metal (Li, Al, Ca and Ti) absorbed graphene with defects for hydrogen storage: first-principles calculations. J Nanosci Nanotechnol 2011;11(12):10624–8.
[19] Chen P, Wu X, Lin J, Tan KL. High H_2 uptake by alkali-doped carbon nanotubes under ambient pressure and moderate temperatures. Science 1999;285(5424):91–3.
[20] Yang RT. Hydrogen storage by alkali-doped carbon nanotubes–revisited. Carbon 2000;38(4):623–6.
[21] Bhat VV, Contescu CI, Gallego NC, Baker FS. Atypical hydrogen uptake on chemically-activated, ultramicroporous carbon. Carbon 2010;48(5):1331–40.
[22] Cabria I, Lopez MJ, Alonso JA. Enhancement of hydrogen physisorption on graphene and carbon nanotubes by Li doping. J Chem Phys 2005;123(20):204721.
[23] Cabria I, Lopez MJ, Alonso JA. Hydrogen storage in pure and Li-doped carbon nanopores: combined effects of concavity and doping. J Chem Phys 2008;128(14):144704.
[24] Kiran B, Kandalam AK, Jena P. Hydrogen storage and the 18-electron rule. J Chem Phys 2006;124(22):224703.
[25] Zhao Y, Kim YH, Dillon AC, Heben MJ, Zhang SB. Hydrogen storage in novel organometallic buckyballs. Phys Rev Lett 2005;94(15):155504.
[26] Durgun E, Jang YR, Ciraci S. Hydrogen storage capacity of Ti-doped boron-nitride and B/Be-substituted carbon nanotubes. Phys Rev B 2007;76(7):073413.
[27] Yildirim T, Ciraci S. Titanium-decorated carbon nanotubes as a potential high-capacity hydrogen storage medium. Phys Rev Lett 2005;94(17):175501.
[28] Kubas GJ. Metal–dihydrogen and σ-bond coordination: the consummate extension of the Dewar–Chatt–Duncanson model for metal–olefin π bonding. J Organomet Chem 2001;635(1):37–68.
[29] Cabria I, Lopez MJ, Alonso JA. Theoretical study of the transition from planar to three-dimensional structures of palladium clusters supported on graphene. Phys Rev B 2010;81(3):035403.
[30] Sun Q, Wang Q, Jena P, Kawazoe Y. Clustering of Ti on a C_{60} surface and its effect on hydrogen storage. J Am Chem Soc 2005;127(42):14582–3.
[31] Krasnov PO, Ding F, Singh AK, Yakobson BI. Clustering of Sc on SWNT and reduction of hydrogen uptake: Ab-initio all-electron calculations. J Phys Chem C 2007;111(49):17977–80.
[32] Lopez I, German E, Juan A, Volpe MA, Brizuela GP. DFT study of hydrogen adsorption on palladium decorated graphene. J Phys Chem C 2011;115(10):4315–23.
[33] Reddy ALM, Ramaprabhu S. Hydrogen adsorption properties of single-walled carbon nanotube—Nanocrystalline platinum composites. Int J Hydrogen Energy 2008;33(3):1028–34.
[34] Kim HS, Lee H, Han KS, Kim JH, Song MS, Park MS, et al. Hydrogen storage in Ni nanoparticle-dispersed multiwalled carbon nanotubes. J Phys Chem B 2005;109(18):8983–6.
[35] Choudhary A, Malakkal L, Siripurapu RK, Szpunar B. Szpunar. First principles calculations of hydrogen storage on Cu and Pd-decorated graphene. Int J Hydrogen Energy 2016;41(39):17652–6.
[36] Zacharia R, Kim KY, Kibria AF, Nahm KS. Enhancement of hydrogen storage capacity of carbon nanotubes via spill-over from vanadium and palladium nanoparticles. Chem Phys Lett 2005;412:369.
[37] Lipson AG, Lyakhov BF, Saunin EI, Tsivadze AY. Evidence for large hydrogen storage capacity in single-walled carbon nanotubes encapsulated by electroplating Pd onto a Pd substrate. Phys Rev B 2008;77(8):081405.
[38] Lee JW, Kim HS, Lee JY, Kang JK. Hydrogen storage and desorption properties of Ni-dispersed carbon nanotubes. Appl Phys Lett 2006;88(14):3126.
[39] Yang FH, Yang RT. Ab initio molecular orbital study of adsorption of atomic hydrogen on graphite: insight into hydrogen storage in carbon nanotubes. Carbon 2002;40(3):437–44.
[40] Yildirim T, Iniguez J, Ciraci S. Molecular and dissociative adsorption of multiple hydrogen molecules on transition metal decorated C_{60}. Phys Rev B 2005;72(15):153403.
[41] Durgun E, Ciraci S, Yildirim T. Functionalization of carbon-based nanostructures with light transition-metal atoms for hydrogen storage. Phys Rev B 2008;77(8):085405.
[42] Dag S, Ozturk Y, Ciraci S, Yildirim T. Adsorption and dissociation of hydrogen molecules on bare and functionalized carbon nanotubes. Phys Rev B 2005;72(15):155404.
[43] Xiao H, Li SH, Cao JX. First-principles study of Pd-decorated carbon nanotube for hydrogen storage. Chem Phys Lett 2009;483(1):111–4.
[44] Lopez I, German E, Juan A, Volpe MA, Brizuela GP, Juan A. Tight-binding study of hydrogen adsorption on palladium decorated graphene and carbon nanotubes. Int J Hydrogen Energy 2010;35(6):2377–84.
[45] Javan MB, Tajabor N, Behdani M, Rokn-Abadi MR. Influence of 3d transition metals (Fe, Co) on the structural, electrical and magnetic properties of C_{60} nano-cage. Phys B Cond Matter 2010;405(24):4937–42.
[46] Javan MB, Ganji MD, Sabet M, Danesh N. Incorporation of hydrogen molecules into carbon nitride heterofullerenes: an Ab initio study. J Comp Theor Nanosci 2011;8(5):803–7.
[47] Javan MB. Fullerene-like $Si_{60}C_{60}$ nanocage: hydrogen storage capacity. Curr Appl Phys 2014;14(3):484–90.
[48] Pham-Huu C, Keller N, Ehret G, Ledoux MJ. The first preparation of silicon carbide nanotubes by shape memory synthesis and their catalytic potential. J Catal 2001;200(2):400–10.
[49] Teo BK, Li CP, Sun XH, Wong NB, Lee ST. Silicon-silica nanowires, nanotubes, and biaxial nanowires: inside,

outside, and side-by-side growth of silicon versus silica on zeolite. Inorg Chem 2003;42(21):6723–8.
[50] Zhao M, Xia Y, Li F, Zhang RQ, Lee ST. Strain energy and electronic structures of silicon carbide nanotubes: density functional calculations. Phys Rev B 2005;71(8):085312.
[51] Zhao M, Xia Y, Zhang RQ, Lee ST. Manipulating the electronic structures of silicon carbide nanotubes by selected hydrogenation. J Chem Phys 2005;122(21):214707.
[52] Mpourmpakis G, Tylianakis E, Froudakis GE. Carbon nanoscrolls: a promising material for hydrogen storage. Nano Lett 2007;7(7):1893–7.
[53] Javan MB. Adsorption of CO and NO molecules on SiC nanotubes and nanocages: DFT study. Surf Sci 2015;635:128–42.
[54] Seyller T. Passivation of hexagonal SiC surfaces by hydrogen termination. J Phys Cond Matter 2004;16(17):S1755.
[55] Styrov VV, Tyutyunnikov VI, Sergeev OT, Oya Y, Okuno K. Chemical reactions of atomic hydrogen at SiC surface and heterogeneous chemiluminescence. J Phys Chem Solids 2005;66(2):513–20.
[56] Pollmann J, Peng X, Wieferink J, Krüger P. Adsorption of hydrogen and hydrocarbon molecules on SiC (001). Surf Sci Rep 2014;69(2):55–104.
[57] Du Y, Xue Q, Zhang Z, Xia F, Liu Z, Xing W. Enhanced hydrogen gas response of Pd nanoparticles-decorated single walled carbon nanotube film/SiO2/Si heterostructure. AIP Adv 2015;5(2):027136.
[58] Gali A. Ab initio theoretical study of hydrogen and its interaction with boron acceptors and nitrogen donors in single-wall silicon carbide nanotubes. Phys Rev B 2007;75(8):085416.
[59] Wang X, Liew KM. Density functional study of interaction of lithium with pristine and Stone-Wales-defective single-walled silicon carbide nanotubes. J Phys Chem C 2012;116(51):26888–97.
[60] Banerjee S, Majumder C. Conformers of hydrogenated SiC honeycomb structure: a first principles study. AIP Adv 2013;3(8):082136.
[61] Song N, Wang Y, Zheng Y, Zhang J, Xu B, Sun Q, Jia Y. New template for Li and Ca decoration and hydrogen adsorption on graphene-like SiC: a first-principles study. Comput Mat Sci 2015;99:150–5.
[62] Barghi SH, Tsotsis TT, Sahimi M. Hydrogen sorption hysteresis and superior storage capacity of silicon-carbide nanotubes over their carbon counterparts. Int J Hydrogen Energy 2014;39(36):21107–15.
[63] Sankey OF, Niklewski DJ. Ab initio multicenter tight-binding model for molecular-dynamics simulations and other applications in covalent systems. Phys Rev B 1989;40(6):3979.
[64] Troullier N, Martins JL. Efficient pseudopotentials for plane-wave calculations. Phys Rev B 1991;43(3):1993.
[65] Kleinman L, Bylander DM. Efficacious form for model pseudopotentials. Phys Rev Lett 1982;48(20):1425.
[66] Perdew JP, Burke K, Ernzerhof M. Generalized gradient approximation made simple. Phys Rev Lett 1996;77(18):3865.
[67] Boys SF, Bernardi FD. The calculation of small molecular interactions by the differences of separate total energies. Mol Phys 1970;19(4):553–66.
[68] Fitts Donald D. Principles of quantum mechanics: as applied to chemistry and chemical physics. Cambridge: Cambridge University Press; 2002. p. 186. ISBN 0-521-65124-7.
[69] Payne MC, Teter MP, Allan DC, Arias TA, Joannopoulos JD. Iterative minimization techniques for ab initio total-energy calculations: molecular dynamics and conjugate gradients. Rev Mod Phys 1992;64:1045.
[70] Kittel C. Introduction to Solid State Physics. New York: Wiley; 1996.
[71] Weast RC, Selby SM. Handbook of Chemistry and Physics. Cleveland, OH: Chemical Rubber Co.; 1974.
[72] Knight LB, Weltner W. Hyperfine interaction and chemical bonding in the PdH molecule. J Mol Spectrosc 1971;40(2):317–27.
[73] Tolbert MA, Beauchamp JL. Homolytic and heterolytic bond dissociation energies of the second row group 8, 9, and 10 diatomic transition-metal hydrides: correlation with electronic structure. J Phys Chem 1986;90(21):5015–22.
[74] Efremenko I, German ED, Sheintuch M. Density functional study of the interactions between dihydrogen and Pd_n ($n = 1–4$) clusters. J Phys Chem A 2000;104(34):8089–96.
[75] Ni M, Zeng Z. Density functional study of hydrogen adsorption and dissociation on small Pd_n ($n = 1–7$) clusters. J Mol Struct THEOCHEM 2009;910(1):14–9.
[76] Blanksby SJ, Ellison GB. Bond dissociation energies of organic molecules. Acc Chem Res 2003;36(4):255–63.
[77] Chan KT, Neaton JB, Cohen ML. First-principles study of metal adatom adsorption on graphene. Phys Rev B 2008;77(23):235430.
[78] Maiti A, Ricca A. Metal–nanotube interactions–binding energies and wetting properties. Chem Phys Lett 2004;395(1):7–11.
[79] Durgun E, Dag S, Bagci VMK, Gülseren O, Yildirim T, Ciraci S. Systematic study of adsorption of single atoms on a carbon nanotube. Phys Rev B 2003;67(20):201401.